Int J Earth Sci (Geol Rundsch) (2016) 105:1881–1899
DOI 10.1007/s00531-016-1298-z

ORIGINAL PAPER

Tracking the late Paleozoic to early Mesozoic margin of northern Gondwana in the Hellenides: paleotectonic constraints from U–Pb detrital zircon ages

Vasileios Chatzaras[1,2] · Wolfgang Dörr[3] · Axel Gerdes[3,4] · Jochen Krahl[5] · Paraskevas Xypolias[6] · Gernold Zulauf[3]

Received: 24 June 2015 / Accepted: 3 January 2016 / Published online: 25 January 2016

Abstract We report new detrital zircon U–Pb ages of nine quartzites sampled along the Phyllite–Quartzite unit sensu stricto (PQ unit s.s.), in the high-pressure belt of the southern Hellenides. The detrital zircon age spectra are dominated by two significant age peaks at ca. 600 and ca. 1000 Ma, which are typical for an east Gondwana provenance. The absence of zircons of Carboniferous–Triassic ages suggests that the depositional environment was isolated from Variscan and early Mesozoic sources. Our data are in support of paleogeographic configurations placing the protolith of the PQ unit s.s. south of the Paleotethys ocean and along the northern Gondwana margin. The zircon age spectra do not show significant variations with respect to the tectonostratigraphic position within the PQ unit s.s. and the position along the high-pressure belt. Combining the new (this study) with published detrital zircon ages, we suggest that the siliciclastic metasediments of the PQ unit s.s. on Crete, Kythera, and the Peloponnesus have a common paleogeographic origin.

Keywords U–Pb zircon geochronology · Detrital zircons · Gondwana · Paleotethys · Peloponnesus · Crete

Electronic supplementary material The online version of this article (doi:10.1007/s00531-016-1298-z) contains supplementary material, which is available to authorized users.

✉ Vasileios Chatzaras
chatzaras@wisc.edu

[1] Department of Geoscience, University of Wisconsin-Madison, Madison, WI 53706, USA

[2] Department of Earth Sciences, Utrecht University, PO Box 80.021, 3508 TA Utrecht, The Netherlands

[3] Institute of Geosciences, Goethe University, Altenhöferallee 1, 60438 Frankfurt Am Main, Germany

[4] Department of Earth Sciences, Stellenbosch University, Private Bag X1, Matieland 7602, South Africa

[5] Agnesstraße 45, 80798 Munich, Germany

[6] Department of Geology, University of Patras, 26500 Patras, Greece

Introduction

Understanding the tectonic evolution of the eastern Mediterranean relies significantly on deciphering the tectonic processes that took place between Gondwana and Eurasia in late Neoproterozoic to early Mesozoic times. Critical aspects are the robust reconstruction of the northern Gondwana margin and the correct identification of the remnants of the peri-Gondwana terranes, which bordered the margin (Murphy et al. 2004). Two major types of peri-Gondwana terranes (Avalonian and Cadomian) have been identified based on the basement age, the provenance of associated sediments, and Nd isotopic signatures (e.g., Nance and Murphy 1996; Stampfli et al. 2002; Samson et al. 2005). In the eastern Mediterranean, the Minoan terranes have been recognized as a separate collection of crystalline complexes related to eastern Gondwana (Zulauf et al. 2007, 2015; Dörr et al. 2015).

During Paleozoic, the rifted fragments from the dismembered belt of the peri-Gondwana terranes moved northward, giving birth first to the Rheic and subsequently to the Paleotethys oceans (e.g., Stampfli and Borel 2002; Stampfli et al. 2002). These Gondwana fragments were accreted to the southern margin of Eurasia and were involved in the late Paleozoic Variscan orogeny (von Raumer 1998; Stampfli and Borel 2002). Late Paleozoic rifting at the northern Gondwana margin induced detachment of the Cimmerian terranes. Continued northward subduction of Paleotethys

below Eurasian lithosphere caused northward drifting of the Cimmerian terranes and opening of the Neotethys in late Permian or Late Triassic times (Robertson et al. 1996; Stampfli and Borel 2002). Accretion of the Cimmerian terranes to the southern Eurasian margin or collision with terranes drifted away from Eurasia led to the Middle–Late Triassic Cimmerian orogeny and the final closure of the Paleotethys (Stampfli and Borel 2002; Zulauf et al. 2015). In eastern Mediterranean, structural and metamorphic overprints of Mesozoic and Cenozoic deformation events further complicate the relationships between the different pre-Alpine crustal fragments.

In the Hellenides orogen, pre-Mesozoic crustal fragments of Cadomian-, Avalonian-, Amazonian-, and Minoan-type affinity have been identified (Romano et al. 2004; Anders et al. 2006; Himmerkus et al. 2007; Zulauf et al. 2007, 2015; Meinhold et al. 2010; Zlatkin et al. 2013; Dörr et al. 2015). Juxtaposition of crustal fragments with such variable provenance requires a complex pre-Alpine tectonic history, possibly involving large-scale lateral displacements along major transcurrent faults (Stampfli et al. 2002). Pre-Alpine basement complexes in the southern Hellenides have been interpreted to represent exotic terranes emplaced from the central Mediterranean region by dextral strike-slip movements during late Paleozoic and/or early Mesozoic (Dornsiepen et al. 2001; Robertson 2006). In this case, the provenance of late Paleozoic to early Mesozoic sediments should be characterized by abrupt lateral changes. Alternatively, amalgamation of rifted Gondwana fragments to the southern margin of Eurasia, followed by Triassic closure of the Paleotethys in the south Aegean region (Stampfli and Borel 2002; Stampfli et al. 2002; Moix et al. 2008; Zulauf et al. 2015), could explain the different stratigraphic and tectonic records of the pre-Alpine basement complexes (Romano et al. 2004; Seidel et al. 2006; Xypolias et al. 2006; Dörr et al. 2015; Zulauf et al. 2015). In this case, we should be able to trace the remnants of the Paleotethys suture in the southern Hellenides.

Based on differences in the magmatic and detrital zircon ages, the Paleotethys suture was recently identified on eastern Crete within a tectonostratigraphic sequence consisting of Carboniferous to Triassic siliciclastic metasediments and pre-Alpine crustal fragments (Zulauf et al. 2015). This finding is in agreement with previous stratigraphic studies, which suggest that the Paleotethys suture zone runs through the Peloponnesus and Crete in the southern Hellenides (Stampfli and Borel 2002; Moix et al. 2008). The existence of the Paleotethys suture within the External Hellenides has also been suggested by Kydonakis et al. (2014) based on detrital zircon data from northern Peloponnesus. However, tracking the lateral continuation of the suture zone has been proven difficult due to strong overprinting by Cenozoic high-pressure/low-temperature (HP/LT) metamorphism and related deformation (e.g., Seidel et al. 1982; Theye et al. 1992; Fassoulas et al. 1994; Doutsos et al. 2000; Xypolias and Doutsos 2000; Zulauf et al. 2002; Chatzaras et al. 2006, 2013a; Xypolias et al. 2008; Jolivet et al. 2010; Marsellos et al. 2010; Klein et al. 2013). The Phyllite–Quartzite unit sensu lato (PQ unit s.l.), which hosts the Paleotethys suture on eastern Crete, is exposed for approximately 600 km along the HP belt of the External Hellenides (Fig. 1). The PQ unit s.l. is characterized by significant along-strike variations in the depositional environment of the constituent siliciclastic metasediments (Robertson 2006), which further obscures the lateral tracking of the suture zone. Lateral variations in the depositional environment could be the result of: (1) transcurrent tectonics; (2) variations in basin morphology affecting paleocurrents; and (3) regionally variable input from different river systems and/or source areas.

In this study, we present data that put constraints on the provenance and the lateral associations of the siliciclastic metasediments included in the PQ unit s.l. The age spectra of detrital zircons provide information for the along-strike configuration of the Gondwana margin and shed more light on the tectonic processes that were active in the Paleotethyan realm.

Geological setting

The siliciclastic metasediments of the PQ unit, which are the focus of the present study, are situated in the External Hellenides (Fig. 1a). The External Hellenides are made up of a series of thrust sheets, which in ascending order comprise: the Plattenkalk, Trypali (exposed only on Crete), PQ unit s.l., Tripolitsa, and Pindos units (Fig. 1b). The Plattenkalk unit comprises a late Carboniferous–Eocene mainly carbonate sequence (Epting et al. 1972) covered by an Early Oligocene calcareous flysch (Bizon and Thiebault 1974). The overlying Trypali thrust sheet consists of an Early Triassic–Early Jurassic sequence of dolomites, evaporates, rauhwackes, and shales (Krahl et al. 1983). The Trypali thrust sheet is overthrust by the PQ unit s.l., which comprises a siliciclastic sequence (Krahl et al. 1983; Zulauf et al. 2002; Robertson 2006; Papanikolaou and Vassilakis 2010). The age of the siliciclastic sequence is middle Carboniferous–Late Triassic, constrained by biostratigraphic data from Crete (Krahl et al. 1983); fossil finds are rare in the Peloponnesus and Kythera. The Tripolitsa and Pindos thrust sheets are mainly composed of Mesozoic carbonate rocks covered by Eocene–Oligocene flysch (Bonneau 1984; Konstantopoulos et al. 2013). The pile of the External Hellenides thrust sheets is overlain by a Neogene–Quaternary sedimentary succession (Fortuin 1978; van Hinsbergen and Meulenkamp 2006; Zachariasse et al. 2011; Maravelis et al. 2013).

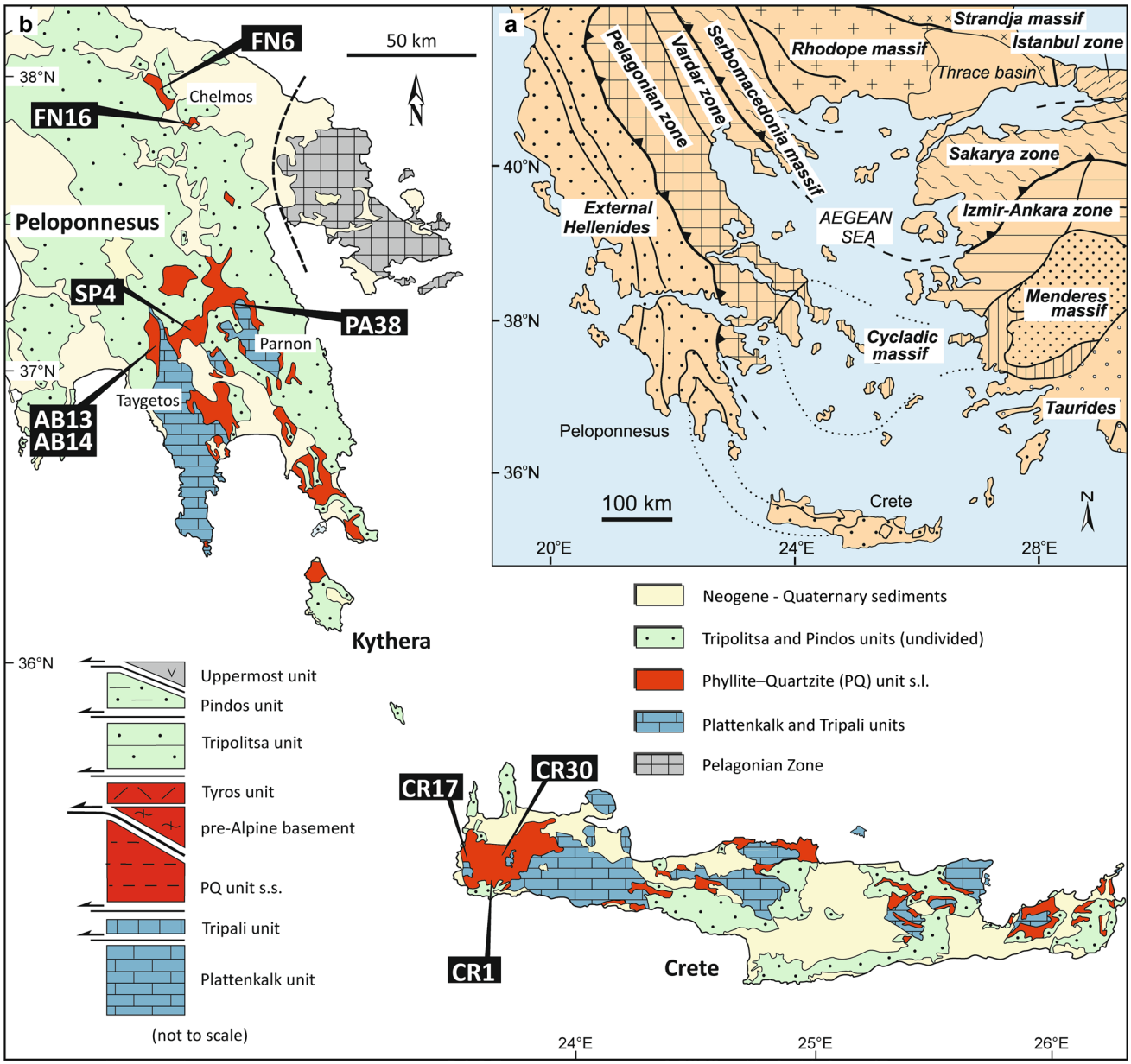

Fig. 1 **a** Map of the major tectonic elements in Greece and western Turkey. **b** Geological map of the External Hellenides. The siliciclastic metasediments analyzed in the present study comprise part of the PQ unit s.l. (in *red*). The internal subdivision of the PQ unit s.l. into PQ unit s.s., pre-Alpine basement, and Tyros unit is shown in the tectonostratigraphic column. The locations of the nine analyzed samples are also shown in the map

The PQ unit s.l. cannot be treated as a single unit; it consists of several internal units with significant differences in protolith age, deformation, as well as in metamorphic age and grade (Zulauf et al. 2002, 2015; Stampfli et al. 2003; Robertson 2006; Papanikolaou and Vassilakis 2010). The structurally lower part is the PQ unit sensu stricto (PQ unit s.s.), which consists of middle Carboniferous–Early Triassic phyllites, quartzites, marbles, and metavolcanics (Krahl et al. 1983, 1986). Under the term PQ unit s.s., we include both the Arna unit of Peloponnesus (Papanikolaou and Skarpelis 1987) and the PQ unit of western Crete (Krahl et al. 1983; Robertson 2006). Detrital zircon age spectra are dominated by Ediacaran and Tonian age peaks at ca. 600 Ma and ca. 1 Ga, respectively (Marsellos et al. 2012; Kydonakis et al. 2014; Dörr et al. 2015). The protolith of the PQ unit s.s. was metamorphosed to HP/LT conditions in late Oligocene, at ca. 24 Ma (Seidel et al. 1982). Peak metamorphic conditions ($T = 450$ °C and $P = 13$–17 kbar) have been reported from the southern Peloponnesus and decrease toward the northern Peloponnesus and eastern

Crete (Katagas et al. 1991; Theye et al. 1992; Blumör 1998; Zulauf et al. 2002; Jolivet et al. 2010).

The PQ unit s.s. is overthrust by the pre-Alpine basement unit, which contains subcomplexes of different protolith age and metamorphic history (Finger et al. 2002; Romano et al. 2006; Seidel et al. 2006; Xypolias et al. 2006; Lode et al. 2008; Zulauf et al. 2008, 2015; Dörr et al. 2015). A Precambrian basement has been identified in the southern Peloponnesus and on eastern Crete, composed of micaschists, quartzites, and meta-graywackes intruded by Cambrian granitoids (511–524 Ma) (Romano et al. 2004; Dörr et al. 2015). On Kythira island, the pre-Alpine basement consists of felsic gneisses, which provide evidence for both Carboniferous to early Permian (323–302 Ma; Xypolias et al. 2006; Seidel et al. 2006) and Late Triassic (232 ± 2 Ma; Lode et al. 2008) plutonism. Moreover, the pre-Alpine basement on eastern Crete underwent amphibolite-facies metamorphism during Carboniferous and Permian, followed by Jurassic cooling (Finger et al. 2002; Romano et al. 2006).

The Tyros unit overlies the pre-Alpine basement and consists of Permian to Late Triassic conglomerates, siliciclastics, carbonates, slates, as well as andesites and felsic volcanic rocks (Krahl et al. 1986; Robertson 2006, 2008; Zulauf et al. 2008, 2013, 2015). Lower Permian and Triassic magmatism, coeval with the deposition of the Tyros sediments, is indicated by the existence of felsic volcanic rocks (285 ± 2, 249 ± 2, 228 ± 1 Ma, concordant U–Pb zircon ages with 2σ uncertainties) and by detrital zircons (242 ± 3, 240 ± 5, 237 ± 3 Ma, concordant U–Pb zircon ages with 2σ uncertainties) separated from the Tyros unit metasediments (Zulauf et al. 2013, 2015). The detrital zircon ages of the Tyros unit further reveal Precambrian and Variscan ages. Triassic magmatism in the pre-Alpine basement and the Tyros unit is consistent with the presence of Triassic felsic plutonic rocks, which are common in different tectonic zones of the Hellenides (e.g., Pelagonia, Cyclades, and Serbomacedonia; Chatzaras et al. 2013b and references therein).

In the Peloponnesus, the distinction between the pre-Alpine basement and the PQ unit s.s. is difficult due to the similarity in the metamorphic temperatures between the Alpine and pre-Alpine deformation (Theye et al. 1992; Gerolymatos 1994; Blumör 1998; Romer et al. 2008). Moreover, the scarcity of fossil finds renders the distinction between the PQ unit s.s. and the Tyros unit in the Peloponnesus difficult but not impossible; the two units are characterized by marked contrasts in their lithologies and metamorphic conditions. The PQ unit s.s. comprises a rock sequence similar to that of Crete, but the Tyros unit is dominated by massive lavas, volcanogenic conglomerates, volcaniclastic sandstones, pink-colored shales, tuffs, quartzitic shales, and micaschists (Gerolymatos 1994; Robertson 2006). The rocks that comprise the Tyros unit have been subjected to low anchimetamorphic conditions of 240–350 °C and 3–6 kbar (Seidel 1978; Thiebault and Triboulet 1984). In contrast, the rocks of the PQ unit s.s. have been subjected to HP/LT metamorphism with estimated conditions of 350–450 °C, 11–13 kbar (Theye 1988) and 450–550 °C, 17 kbar (Theye and Seidel 1991).

The variations in the metamorphic conditions as well as in the magmatic and detrital zircon ages among the constituent units of the PQ unit s.l. indicate a complex paleotectonic evolution that could be associated with an active margin. The existence of a Carboniferous to Permian Variscan active margin within the External Hellenides is documented by: (1) the Carboniferous and Permian metamorphism of the pre-Alpine basement (Finger et al. 2002; Romano et al. 2006); (2) the Carboniferous magmatism in the pre-Alpine basement (Xypolias et al. 2006; Seidel et al. 2006); (3) the tectonostratigraphic relationships described from the Tyros unit on eastern Crete suggesting a major tectonic event in late Carnian–early Norian (Stampfli et al. 2003); and (4) the Carboniferous and Permian detrital zircons in the pre-Alpine basement and the Tyros unit (Zulauf et al. 2015). It has been suggested that in this paleotectonic context, the pre-Alpine basement and the Tyros unit resided above the northward subducting Paleotethys ocean (Stampfli et al. 2003; Stamfli and Kozur 2006; Kydonakis et al. 2014; Zulauf et al. 2015). In contrast, the protolith of the PQ unit s.s. (comprising either both the Arna unit and the PQ unit of western Crete, or only the latter) was situated in the southern Paleotethyan realm (Stampfli et al. 2003; Stamfli and Kozur 2006; Kydonakis et al. 2014; Dörr et al. 2015; Zulauf et al. 2015) as suggested by: (1) the lack of evidence for Variscan age magmatism and metamorphism and (2) the predominance of Ediacaran and Tonian detrital zircons in the protolith of the PQ unit s.s. (Marsellos et al. 2012; Kydonakis et al. 2014; Dörr et al. 2015), which is typical for sequences with provenance from east Gondwana (e.g., Zulauf et al. 2007). We should note that the polarity of the Paleotethys subduction, the position of the Paleotethys suture in the Aegean region, and the nature of the Triassic magmatism are still highly debated. Southward subduction of the Paleotethys ocean beneath the northern Gondwana margin during the late Paleozoic–early Mesozoic has been suggested by Şengör et al. (1984), Romano et al. (2006), and Xypolias et al. (2006). In the case of a northward subducting Paleotethys ocean, occurrence of the Paleotethys suture in more internal (northern) parts of the Hellenides orogen has been suggested by Robertson et al. (1996) and Robertson (2007). Depending on the tectonic model, the Triassic magmatism could be either rift- or subduction-related. Recent O-Hf isotopic compositions of zircons suggest that Triassic magmatism is more likely rift-related (Fu et al. 2015).

The occurrence of the Paleotethys suture within the southern Hellenides has primarily been proposed based on information from eastern Crete (Stampfli et al. 2003; Zulauf et al. 2015) and northern Peloponnesus (Kydonakis et al. 2014). Tracing the Paleotethys suture along the HP belt, however, requires determining the provenance of the metamorphosed siliciclastic sequences that have collectively been grouped together as PQ unit s.l. Detrital zircon dating comprises a powerful tool for unraveling the paleogeographic configuration of the siliciclastic sequences in the External Hellenides in the context of the tectonic evolution of eastern Mediterranean.

Analytical methods

Petrographic and microstructural analyses

Thin sections of siliciclastic metasediments collected for U–Pb zircon dating were investigated for accessory minerals, detrital rock fragments, and inherited deformation microstructures in the detrital quartz and feldspar grains. The microscopic observations are used to constrain the source rock type and the grade of metamorphic temperature in the source area.

Laser ablation (LA)-ICP-MS method

Samples for isotope mass spectrometry were processed at the Institut für Geowissenschaften of Frankfurt University using standard mineral separation techniques. These include crushing and sieving, before concentration of heavy minerals by heavy liquids (bromoform, methylene iodide) and magnetic separation with a Frantz isodynamic separator. Hand-picked zircon grains were mounted in 25-mm-diameter circular epoxy mounts and polished to expose the grain interior. Prior to their analysis, the grains were examined using cathodoluminescence (CL) imaging in order to recognize their internal structure and to identify cracks and mineral inclusions. Zircon U–Pb isotope analysis was performed by LA-ICP-MS technique using a Thermo Finnigan Element II sector field ICPMS attached to a New Wave LUV213 laser ablation system ($\lambda = 213$ nm). Ablation was carried out in a He carrier gas in a low volume (2.5 cm^3) cell; laser beam parameters used were 30 μm diameter; 5 Hz repetition rate; and 75 % power output. Isotope data were acquired in peak-jumping mode on eight masses; ^{202}Hg, ^{204}Pb, ^{206}Pb, ^{207}Pb, ^{208}Pb, ^{235}U, and ^{238}U. Background and ablation data for each analysis were collected over 90 s, with background measurements (carrier gas, no ablation) being taken over the first 30 s prior to initiation of ablation. The data were collected at time-resolved mode allowing acquisition of the signal as a function of time (ablation depth) and subsequently recognition of isotopic heterogeneities within the ablated volume. Raw data were processed offline using an Excel® spreadsheet program (Frei and Gerdes 2008). Mass discrimination and elemental fractionation during laser ablation were corrected by calibration against the GJ-1 zircon standard (Jackson et al. 2004), which was analyzed routinely during analytical sessions (three standard analyses at the beginning and end of every session of 33 unknowns, and two standard analyses every 10 unknowns). Prior to this correction, the change of elemental fractionation (e.g., Pb/U and Pb/Th ratios as function of ablation time and thus depth) was corrected for each set of isotope ratios by applying a linear regression through all measured ratios versus time, excluding outliers (>2 s.e.), and taking the intercept $t = 0$ as the correct ratio. Changes in isotopic ratios arising from laser drilling into domains of distinct Pb/U ratio (core/rim), mineral inclusions, and zones affected by Pb loss (metamictization/cracks) can usually be detected by careful monitoring of the time-resolved signal, and such analyses are rejected. Common Pb correction was applied only when the interference- and background-corrected ^{204}Pb signal were significantly higher than the detection limit of about 20 cps. The latter is limited by the amount of Hg in the carrier gas and the accuracy to which the ^{202}Hg and thus the interfering ^{204}Hg can be monitored. Corrections made are based on common Pb composition given by the second-stage growth curve of Stacey and Kramers (1975) for Neoproterozoic age (600 Ma). Data presentation was made with Isoplot (Ludwig 1994). In order to monitor the reproducibility and accuracy of our analytical procedure, zircon reference standard materials 91,500 (Wiedenbeck et al. 1995), Plešovice (Sláma et al. 2008) and M 257 (Nasdala et al. 2008) were analyzed, and the results were consistently in excellent agreement with the published ID-TIMS data. The homogeneity of measured zircon reference standard materials was verified by ID-TIMS analyses. The laser-ICP-MS U–Pb data of the detrital zircons are reported with 2σ uncertainties in Table 1 (Supplementary data).

Sample description, petrography, and microstructure

We collected nine quartzite samples from western Crete (3 samples), central Peloponnesus (4 samples), and northern Peloponnesus (2 samples) along the PQ unit s.s. (Fig. 1; Table 2, Supplementary data). Sampling covers in plan-view a 400-km-long segment of the PQ unit s.s. and allows studying lateral variations in the detrital zircon ages and the source area. The age of the sampled quartzites was constrained only on western Crete, on the basis of existing biostratigraphic data; age determination was difficult for

the Peloponnesus due to the scarcity of preserved fossils in the siliciclastic metasediments. The locality, tectonostratigraphic position, and age (where possible) of the analyzed samples are described below, along with their petrographic and microstructural characteristics.

Northern Peloponnesus

In the northern Peloponnesus, two quartzite samples (FN6 and FN16) were collected from the Chelmos tectonic window (Fig. 1b). The samples were situated approximately 125 m (FN16) and 800 m (FN6) below the tectonic contact between the Tyros and PQ unit s.s. (Xypolias and Doutsos 2000; their figs. 3a, 5); pre-Alpine basement has not been recognized in the Chelmos window. Xypolias and Doutsos (2000) and Xypolias and Koukouvelas (2001) have previously studied Alpine deformation in the two quartzites. It should be noted that sample FN6 was situated at structural distance ca. 100 m above the quartzite sample analyzed for detrital zircon ages by Kydonakis et al. (2014). Therefore, the two samples analyzed in this study augment the existing detrital zircon dataset in the northern Peloponnesus and provide information for detrital zircon provenance at higher structural levels of the PQ unit s.s., compared to the study of Kydonakis et al. (2014). The quartzites show a strong foliation, which results from stretched quartz grains and the shape-preferred orientation of white mica (Fig. 2a). The maximum size of the detrital quartz grains is 0.5 mm, and the grains do not show significant inherited internal deformation. The few albite porphyroclasts contained in the quartzites are up to 2 mm in size and show internal foliation, which is oblique to the dominant external foliation (Fig. 2a). Accessory minerals are tourmaline, titanite, zircon, and opaque phases.

Central Peloponnesus

Four quartzites were sampled across the PQ unit s.s. in central Peloponnesus (Fig. 1b). Sample PA38 was collected from the Parnon tectonic window, approximately 300 m above the basal thrust carrying the 2000 m thick PQ unit s.s. on the Plattenkalk unit. Sample PA38 comes from the same sampling locality as sample PA39 of Xypolias and Kokkalas (2006; their fig. 3). The quartzite is foliated and consists of detrital quartz grains, up to 0.5 mm in size. Plagioclase is restricted to discrete layers, which are aligned parallel to the main foliation.

Three quartzite samples were collected from the Taygetos tectonic window (Fig. 1b). Samples AB13 and AB14 were collected 350–370 m above the basal thrust carrying the ca. 1500 m thick PQ unit s.s. on the Plattenkalk unit (Xypolias and Kokkalas 2006; their fig. 2). Sample SP4 (Doutsos et al. 2000; their fig. 4a) was collected from a higher structural position compared to samples AB13 and AB14; however, its exact distance from the base or the top of the PQ unit s.s. is not well constrained. The quartzites are characterized by strong foliation, resulting from stretched quartz grains and the alignment of white mica. The detrital quartz grains have a maximum size of 0.8–1.5 mm in the analyzed samples. The two samples (AB13 and AB14) representing a lower lithostratigraphic position contain detrital quartz grains with inherited intracrystalline deformation; perpendicular sets of subgrains, resulting in the so-called chessboard pattern (Fig. 2b). The chessboard-type subgrains result from subgrain boundaries, which are parallel to the prim and the basal planes of quartz crystal. Subgrain boundaries aligned parallel to the basal planes result from prism-c-slip, which is restricted to $T > 650$ °C (Passchier and Trouw 2005, and references therein). Alpine deformation of the PQ uint s.s. is typically characterized by lower metamorphic temperatures. The detrital grains may also contain exsolved rutile needles (Fig. 2c).

Sample (SP4) represents a higher lithostratigraphic position and contains detrital quartz, plagioclase, and K-feldspar (less frequently) grains with sizes up to 0.6 mm (Fig. 2d). The lack of significant inherited intracrystalline deformation in the detrital quartz grains and the relatively large amount of detrital plagioclase and K-feldspar suggest the presence of relatively undeformed granite in the source area.

Western Crete

Three quartzites were sampled from the PQ unit s.s. on western Crete (Fig. 1b). Sample CR30 represents the lower tectonostratigraphic position and was collected approximately 20 m above the thrust fault that carries the PQ unit s.s. over the Trypali unit. The quartzite belongs to the upper Permian–Early Triassic "Rambi-Seli slates" formation (Krahl et al. 1983). Sample CR17 was collected from the "Lower Quartzite" formation, of suggested Early Triassic age (Krahl et al. 1983). The sample was collected approximately 50 m above the tectonic contact between the PQ unit s.s. and the Trypali thrust sheet. Sample CR1 occupies a higher tectonostratigraphic position and was collected approximately 70 m below the thrust fault carrying the Tripolitsa unit on the PQ thrust sheet. Sample CR1 was situated beneath the "Mana" formation, which is of Upper Triassic age (Krahl et al. 1983). The sample belongs to the "Upper Quartzite" formation of Krahl et al. (1983); the age of the Upper Quartzite formation is unknown. Marsellos et al. (2012) provide detrital zircon ages for a quartzite also collected from the Upper Quartzite formation (A. Marsellos, pers. comm.). However, the sample of Marsellos et al. (2012) comes from the eastern margin of the Paleochora salient, while our samples from the central

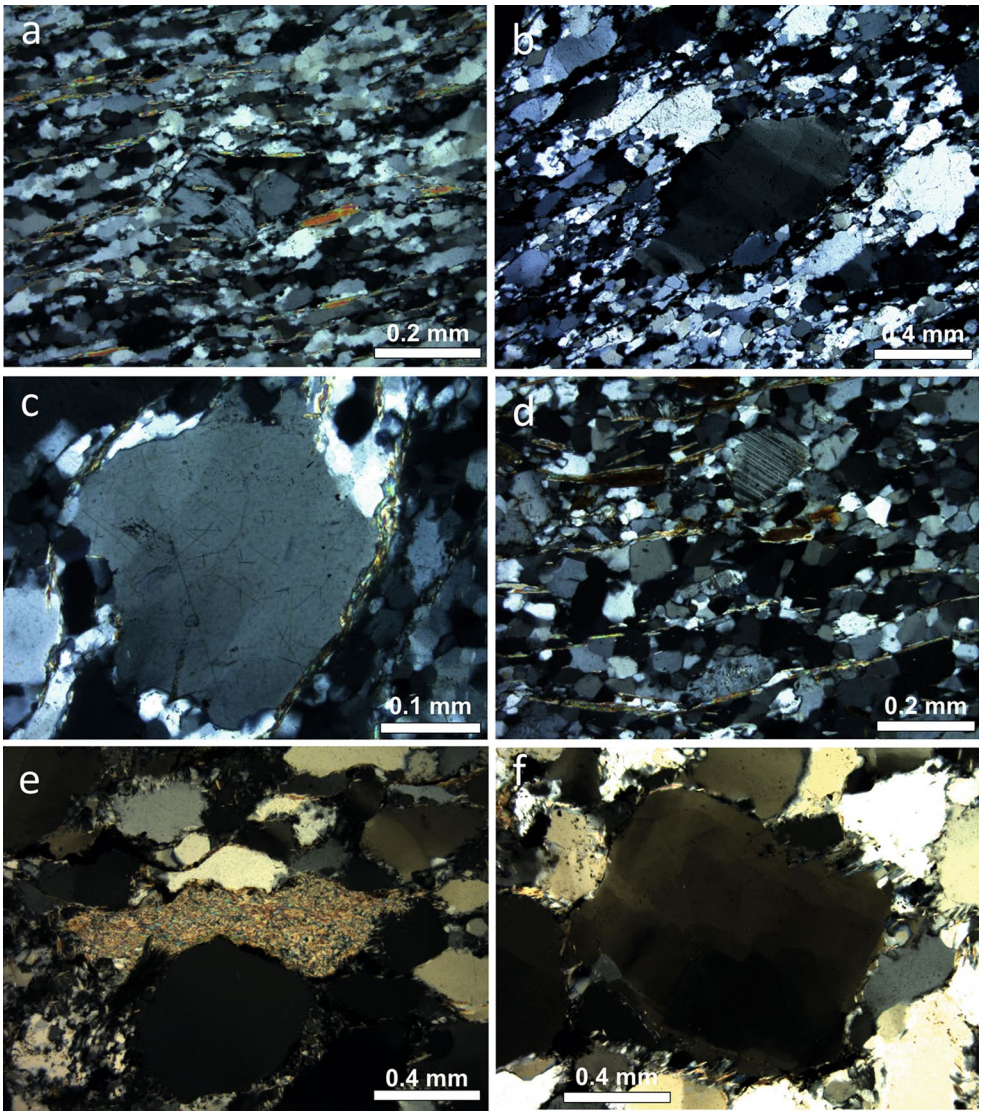

Fig. 2 Microphotographs of siliciclastic metasediments collected from the Peloponnesus and western Crete. All photographs are taken under crossed polarizers. **a** Albite clast in foliated matrix of largely recrystallized quartz and white mica; sample FN16, northern Peloponnesus, Chelmos tectonic window. **b** Detrital quartz grain with perpendicular sets of subgrain boundaries resulting in the so-called chessboard pattern; sample AB14, central Peloponnesus, Taygetos tectonic window. **c** Exsolved rutile needles inside detrital quartz; sample AB14, Taygetos tectonic window. **d** Detrital plagioclase and K-feldspar in matrix of detrital and recrystallized quartz grains; sample SP4, central Peloponnesus, Taygetos tectonic window. **e** Detrital phyllite grain surrounded by detrital quartz grains; sample CR17, western Crete. **f** Detrital quartz grain with perpendicular sets of subgrain boundaries resulting in the "chessboard pattern"; crossed polarizers; sample CR17, western Crete

domain and western margin of the salient (Chatzaras et al. 2013a). Therefore, the three samples analyzed in this study add to the existing detrital zircon dataset in western Crete and provide information for detrital zircon provenance at lower structural levels and laterally distinct parts of the PQ unit s.s., compared to the study of Marsellos et al. (2012).

Samples CR30 and CR1 have common microstructural characteristics. They have strong foliation, formed by the shape-preferred orientation of white mica and quartz grains. Detrital quartz grains are usually monocrystalline and have a size up to 2 mm. Inherited intracrystalline deformation features in the detrital quartz grains are largely lacking, which may suggest that the quartz grains were almost undeformed when being deposited. Sample CR17 from the lower Triassic quartzites contains poorly sorted detrital quartz grains that vary in size from 0.1 to 1.5 mm. Apart from quartz, the quartzite contains phyllite clasts with opaque phases aligned parallel to the phyllitic foliation (Fig. 2e). Inherited intracrystalline deformation of the quartz grains involves the formation of the chessboard pattern of subgrain boundaries (Fig. 2f).

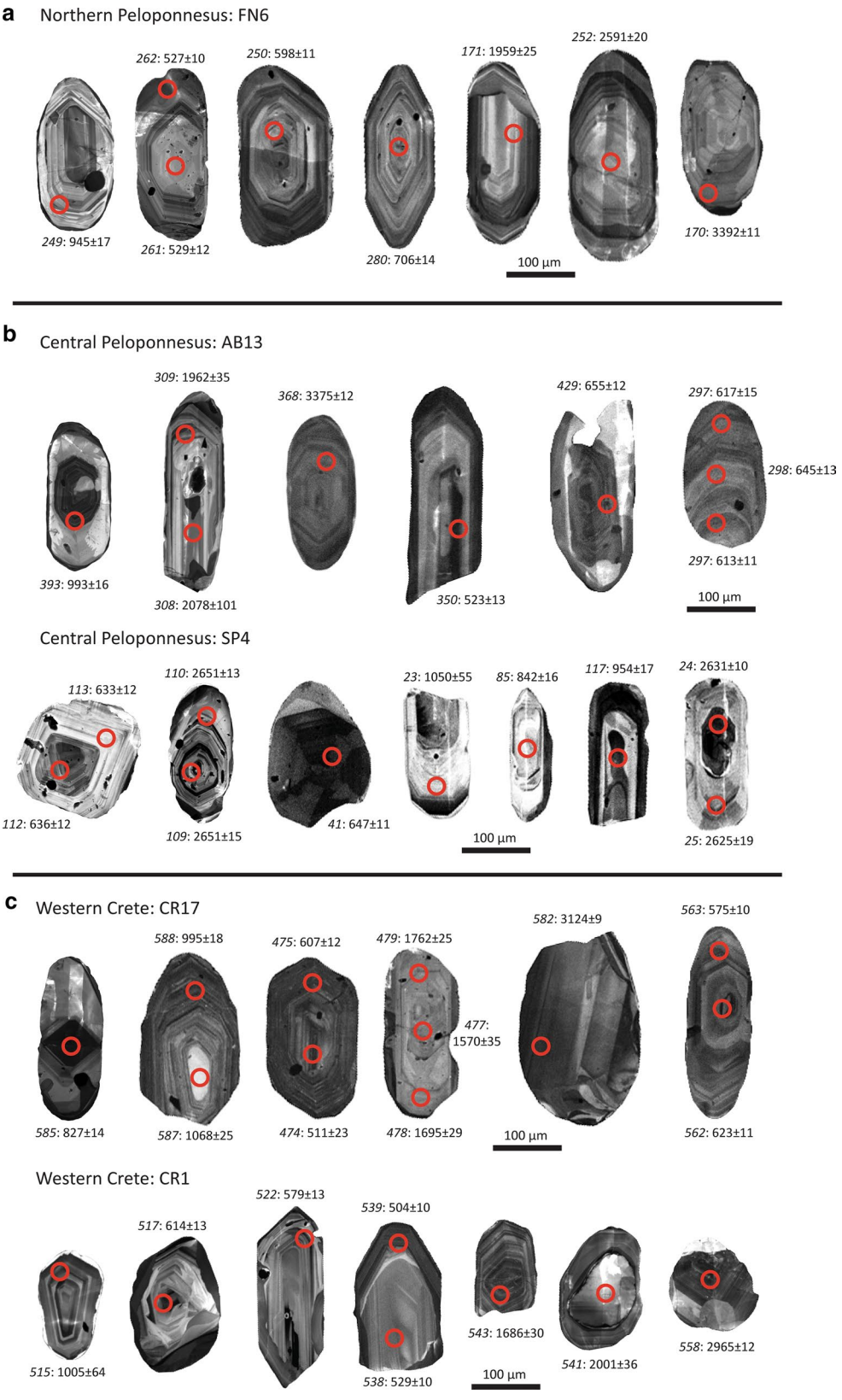

Fig. 3 CL images of selected zircon grains with their corresponding $^{238}U/^{206}Pb$ (younger than 1000 Ma) and $^{207}Pb/^{206}Pb$ (older than 1000 Ma) ages

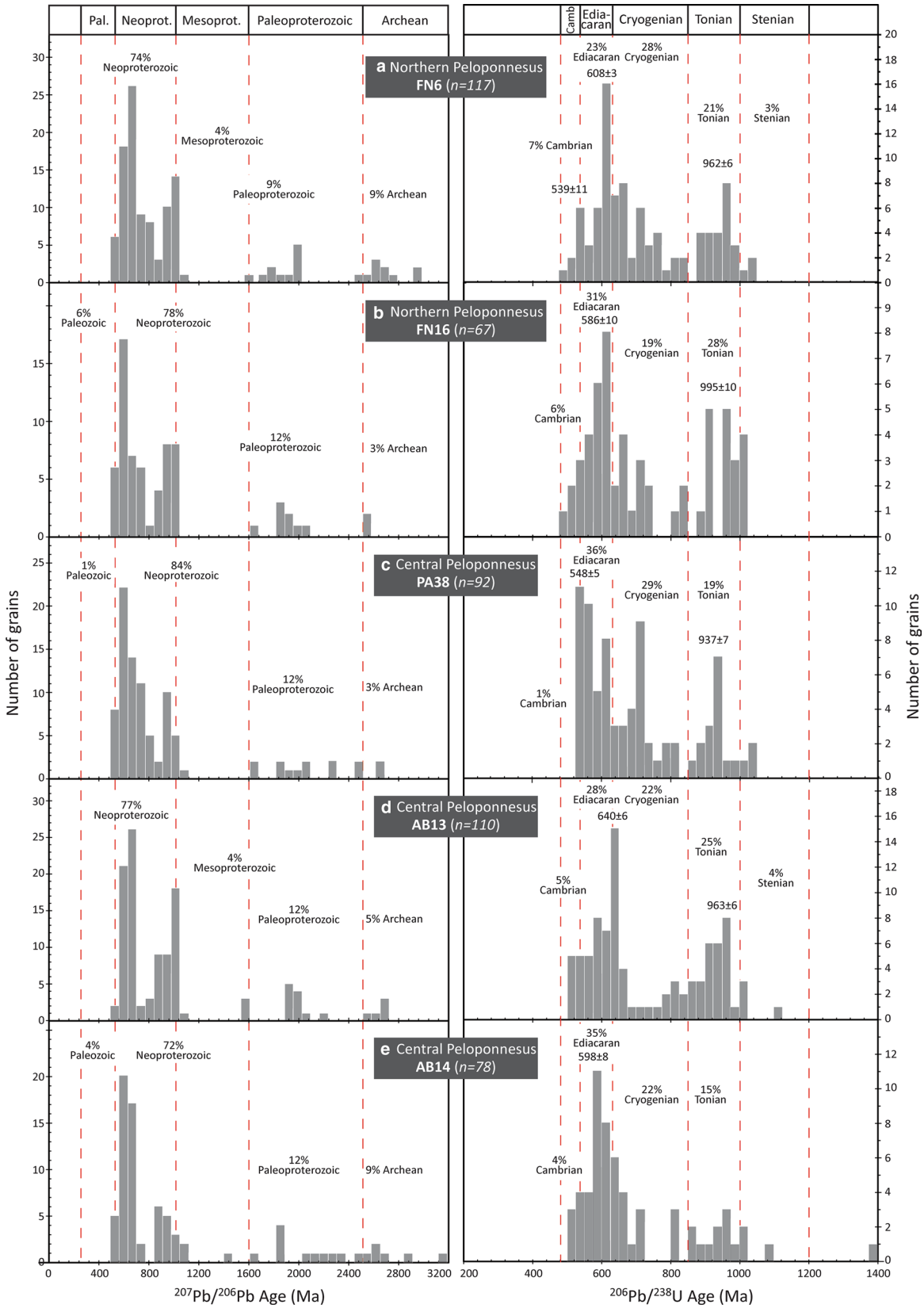

Fig. 4 Histograms of detrital zircons from siliciclastic metasediments of the PQ unit s.s. in northern Peloponnesus (**a**, **b**), central Peloponnesus (**c**–**f**), and western Crete (**g**–**i**). Frequency bars: 91–109 % concordance of the zircon age; *left column* $^{207}Pb/^{206}Pb$ ages for all zircons of a sample; *right column*: $^{206}Pb/^{238}U$ ages for zircons <1.0 Ga

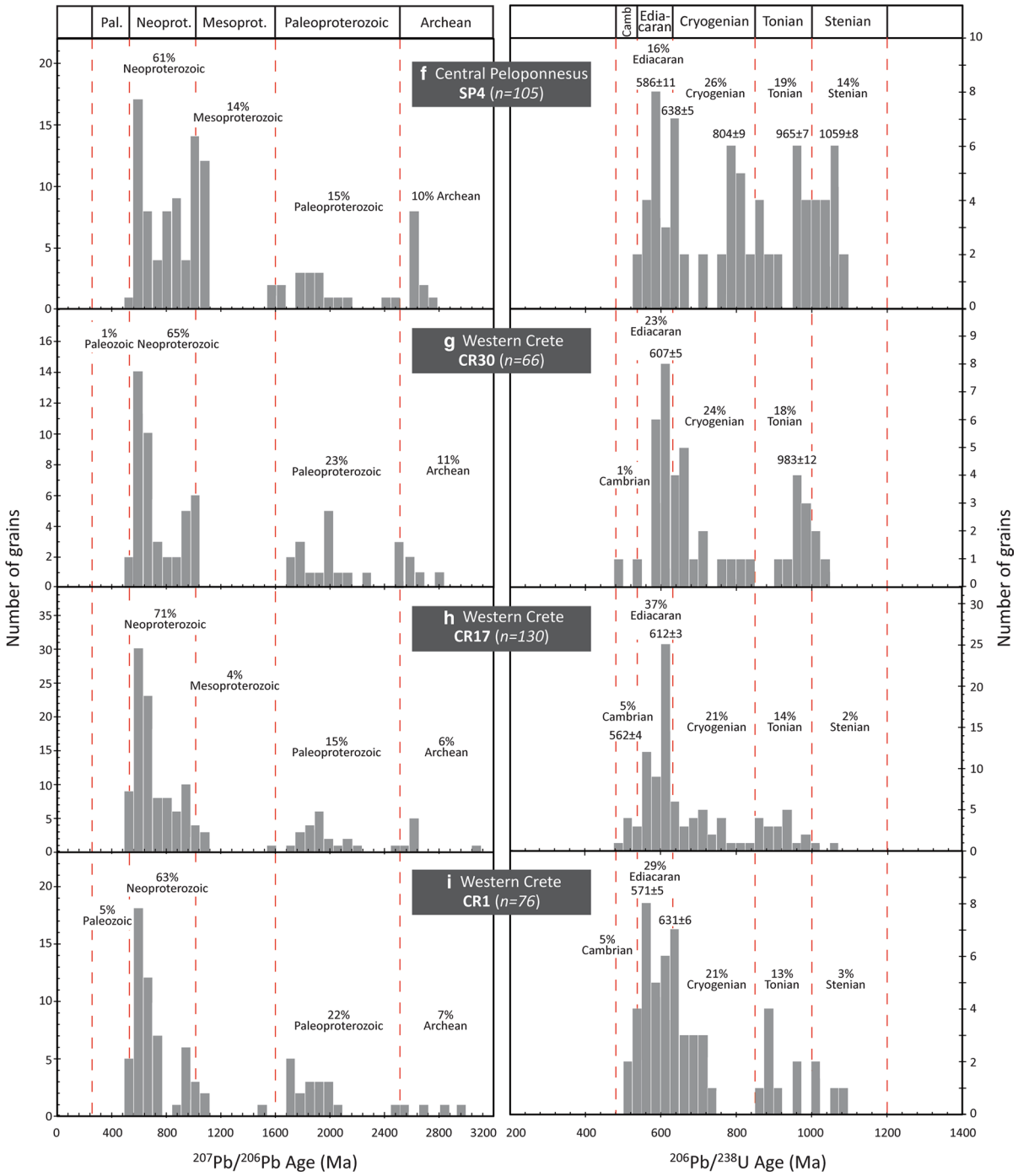

Fig. 4 continued

U–Pb geochronology results

The LA-ICP-MS U–Pb data of the detrital zircons are reported with 2σ uncertainties in Table 1. The CL images of representative zircon types are shown in Fig. 3. The U–Pb results are presented on histogram plots in Fig. 4. For ages younger than 1 Ga, we plot analyses indicating a 91–109 % concordance as ^{238}U–^{206}Pb ages. For the whole sample, we report ^{207}Pb–^{206}Pb ages.

Northern Peloponnesus

The two quartzites collected from the Chelmos tectonic window contain zircons with grain size ranging from 100

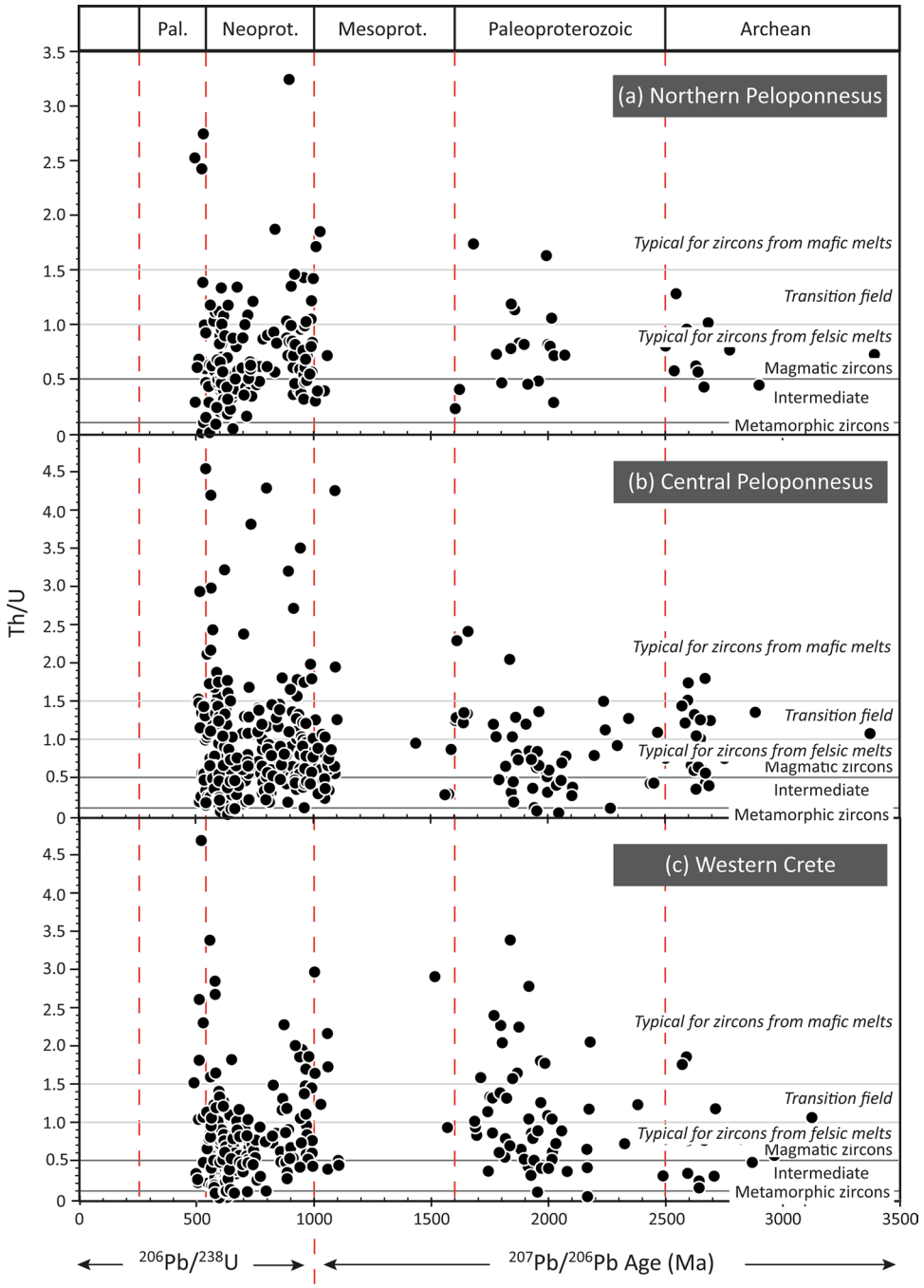

Fig. 5 Zircon Th/U ratio versus age plot for the analyzed PQ unit s.s. quartzites. Samples are grouped based on their locality in plots for **a** northern Peloponnesus, **b** central Peloponnesus, and **c** western Crete. The magmatic versus metamorphic zircon fields are from Teipel et al. (2004). The fields for mafic versus felsic melt sourced zircons are from Linnemann et al. (2011)

to 400 μm. Only 3 % of the zircons are euhedral (Fig. 3a). Most of the zircons (62 %) have a rounded shape, while 35 % are angular (Fig. 3a).

In the structurally lower quartzite (FN6), each of the Archean and Paleoproterozoic zircon groups comprises 9 % of the total zircon population (Fig. 4a). Only 4 grains (3 %) are Mesoproterozoic (Stenian) in age. The age spectrum of the detrital zircons is dominated by Neoproterozoic ages (74 %). The Neoproterozoic zircon group is split into three subgroups of similar size (21 % Tonian, 28 % Cryogenian, and 23 % Ediacaran; Fig. 4a). Cryogenian ages do not show any distinct peak. Conversely, Tonian and Ediacaran peaks occur at 962 ± 6 and 608 ± 3 Ma, respectively. Cambrian zircons (7 %) comprise the younger age group, showing a peak at 539 ± 11 Ma.

Quartzite FN16, which was collected from the upper structural levels of the PQ unit s.s., contains only 3 % Archean and 12 % Paleoproterozoic zircons (Fig. 4b). The age spectrum of the detrital zircons is dominated by Neoproterozoic ages (78 %). The Ediacaran (31 %) and Tonian (28 %) zircons form the two larger groups of Neoproterozoic zircons, with peaks at 586 ± 10 and 995 ± 10 Ma, respectively (Fig. 4b). Cryogenian (19 %) and Cambrian (6 %) zircons do not show any age peak.

In the two quartzites from the northern Peloponnesus, only 3 % of the zircon grains have Th/U ratio equal to 0.1 (Fig. 5a), which has been described as the upper bound for metamorphic grown zircons (Hartmann and Santos 2004). The zircons with Th/U ratio equal to 0.1 are of Cambrian, Ediacaran, and Cryogenian age. The majority of the zircon population (66 %) has Th/U ratio higher than 0.5, which is considered to be typical for magmatic zircons (Teipel et al. 2004), while 93 % of zircons have Th/U ratio lower than 1.5. Values of Th/U ratio lower than 1.5 may indicate potential crystallization from felsic and/or intermediate magmas (Fig. 5a).

Central Peloponnesus

Zircon grains in the four quartzites from the Parnon and Taygetos tectonic windows range in size from 60 to 330 μm. Only 4–14 % of the zircons are euhedral (Fig. 3b). Most of the zircons (52–61 %) have a rounded shape, while 29–44 % are angular.

Sample PA38 from the Parnon window contains 3 % Archean and 12 % Mesoproterozoic zircons. Neoproterozoic ages (84 %) dominate the age spectrum of the detrital zircons; the observed amount of Neoproterozoic zircons is the highest among the studied samples. The Neoproterozoic zircon group is split into three subgroups (19 % Tonian, 29 % Cryogenian, and 36 % Ediacaran; Fig. 4c), with corresponding age peaks at 937 ± 7, 711 ± 7, and 548 ± 5 Ma, respectively.

Quartzite AB13 from the lower structural levels of the PQ unit s.s. in the Taygetos tectonic window contains low amounts of Archean (5 %), Paleoproterozoic (12 %), and Mesoproterozoic (4 %; Stenian) zircons (Fig. 4d). The zircon age spectrum is dominated by a Neoproterozoic age group (77 %), which is split into three equally populated subgroups (25 % Tonian, 22 % Cryogenian, and 28 % Ediacaran; Fig. 4d). Cryogenian ages show no peak. Conversely, peaks of Tonian and Ediacaran ages occur at 963 ± 6 and 640 ± 6 Ma, respectively. The youngest zircons are Cambrian in age and do not show any age peak.

Sample AB14, which is also collected from the base of the PQ unit s.s., contains 9 % of Archean, 12 % of Paleoproterozoic, and 3 % of Mesoproterozoic zircons (Fig. 4e). Neoproterozoic zircons comprise the dominant age group (72 %). The Tonian (15 %) and Cryogenian (22 %) zircons do not show any age peaks, whereas the Ediacaran zircons (35 %) have a prominent peak at 598 ± 8 Ma. The youngest age group represents slightly discordant analyses at 510 ± 10 to 517 ± 12 Ma and comprises part of a small group (4 %) of Cambrian zircons (Fig. 4e).

Quartzite SP4 collected at the upper structural levels of the PQ unit s.s. in the Taygetos window has an age spectrum of detrital zircons different from the samples at the deeper structural levels. Sample SP4 contains the highest amount of Archean (10 %) and Paleoproterozoic (15 %) zircons among all the Peloponnesus samples (Fig. 4f). The group of Archean zircons has an age peak at 2652 ± 13 Ma. The sample also contains the highest amount of Mesoproterozoic zircons (14 %) among all the analyzed samples. The Mesoproterozoic zircons are Stenian and show an age peak at 1059 ± 8 Ma. The Neoproterozoic zircons (61 %) dominate, however, the determined population is the smallest among the analyzed samples. The Cryogenian (26 %) zircons form the largest subgroup of the Neoproterozoic zircons, with two peaks at 804 ± 9 and 638 ± 5 Ma (Fig. 4f). The Tonian (19 %) and Ediacaran (16 %) zircons comprise two almost equally populated subgroups with peaks at 965 ± 7 and 586 ± 11 Ma (Fig. 4f). The determined population of Ediacaran zircons is the smallest among the analyzed samples.

In the four samples collected from the central Peloponnesus, 71 % of the analyzed zircons have Th/U ratio higher than 0.5, while 85 % of zircons have Th/U ratios lower than 1.5 (Fig. 5b). Only 2 % of the analyzed zircons have Th/U lower than 0.1.

Western Crete

Zircon grains in the four quartzites from western Crete range in size from 70 to 430 μm. Only 9 % of the zircons are euhedral (Fig. 3c). Most of the zircons (52–64 %) have rounded shape, while 27–40 % are angular.

The structurally deeper quartzite (CR30) of upper Permian–lower Scythian age contains 11 % Archean and 23 % Paleoproterozoic zircons (Fig. 4g); these are the largest Archean and Paleoproterozoic populations observed among the analyzed samples. The zircon age spectrum is dominated by a Neoproterozoic age group (65 %), which is split into three subgroups (Fig. 4g). The Tonian zircons comprise the smallest of the three subgroups (18 %) and show an age peak at 983 ± 12 Ma. The sample contains an equal amount of Cryogenian (24 %) and Ediacaran (23 %) zircons. The Cryogenian subgroup does not show an age peak, whereas the Ediacaran subgroup has a peak at 607 ± 5 Ma. The younger zircon defines a concordant age at 497 ± 10 Ma (Fig. 5g) and is the only Cambrian zircon found in the quartzite.

The middle–upper Scythian quartzite (CR17) contains 6 % Archean, 15 % Paleoproterozoic, and 4 % Mesoproterozoic zircons (Fig. 4h). The Neoproterozoic zircons dominate the age spectrum. The Tonian (14 %) and Cryogenian (21 %) subgroups do not show age peaks. In contrast, Ediacaran zircons (37 %) display a prominent peak at 612 ± 3 Ma and a minor peak at 562 ± 4 Ma. Cambrian zircons (5 %) comprise the younger age group in the sample (Fig. 4h).

Sample CR1, collected at the higher structural levels of the PQ unit s.s. on western Crete, contains 7 % Archean, 22 % Paleoproterozoic, and only 3 % Mesoproterozoic (Stenian) zircons (Fig. 4i). The zircon age spectrum is dominated by a Neoproterozoic age group (63 %), which contains three subgroups (Fig. 4i). Tonian zircons (13 %) do not show any age peak. Cryogenian (21 %) and Ediacaran (29 %) zircons, however, have age peaks at 631 ± 6 and 571 ± 5 Ma, respectively. Zircons of Cambrian (5 %) age comprise the youngest group in the sample (Fig. 4i).

In the three quartzites from western Crete, the Th/U ratio is larger than 0.5 in 68 % of the analyzed zircons, lower than 1.5 in 81 % of zircons, and lower than 0.1 in only 5 % of zircons (Fig. 5c). Zircons with Th/U ratio lower than 0.1 have either Paleoproterozoic or Neoproterozoic age.

Discussion

Provenance of the detrital zircons

The Th/U ratio can potentially provide information for the magmatic versus metamorphic zircon origin (e.g., Williams et al. 1996; Rubatto et al. 2001). Low Th/U ratios (typically <0.1), characteristic of metamorphic zircons, appear to be limited in our dataset. More than 95 % of the analyzed zircons in each sample are interpreted to have magmatic origin. However, the use of Th/U ratio as a discriminator of zircon origin should be used with caution; metamorphic zircons with high Th/U ratio have been documented (e.g., Möller et al. 2002; Kirkland et al. 2015). The Th/U ratio can be strongly influenced by the bulk-rock composition and by the partitioning behavior of Th and U between zircon grains and coexisting minerals and volatiles (e.g., Harley and Kelly 2007). The Th/U ratio could potentially be indicative of the composition of the magma from which zircons crystallized. The large amount (81–93 %) of detrital zircons with Th/U ratio lower than 1.5 could indicate formation from felsic and intermediate magmas. The analyzed quartzites from the PQ unit s.s. contain mainly detrital monocrystalline quartz grains as well as detrital plagioclase and K-feldspar grains, which suggests that granitoids were exposed in the source area. Therefore, the detritus record in the analyzed samples supports the interpretations from the Th/U ratios.

Some of these granitoids underwent deformation during cooling and exsolution of rutile needles in the detrital quartz grains. High-temperature deformation is indicated by the chessboard pattern of quartz subgrains observed as inherited pre-Alpine structures in the detrital quartz grains. The presence of detrital phyllite clasts in one of the investigated samples suggests that a greenschist-facies basement was also present in the source area. It is therefore possible that felsic granitoids intruded synkinematically into this greenschist-facies basement. A similar pattern, with fragments of very low grade to low-grade rocks, has been observed on eastern Crete at the upper part of the Tyros unit (Dörr et al. 2015). In the upper part of the Tyros unit in eastern Crete, pre-Variscan detritus dominates and is related to the Cadomian and Grenvillian basement of the Cimmerian continent, which derived from east Gondwana.

In Fig. 6c, we combine the new U–Pb zircon ages of the present study with published U–Pb detrital zircon ages from Marsellos et al. (2012), Dörr et al. (2015), and Zulauf et al. (this volume). All the detrital zircon ages are from samples which have been collected from the PQ unit s.s. The age spectra are dominated by Neoproterozoic zircons and are characterized by prominent Ediacaran and Cryogenian age clusters. A significant Stenian/Tonian cluster is also present. The ratio of the Ediacaran peak to Stenian/Tonian peak is approximately 2:1. Typical for the detrital zircon age spectra in the PQ unit s.s. is an age gap between 1.1 and 1.6 Ga. A similar gap in U–Pb zircon ages has also been recorded for siliciclastic metasedimentary rocks of the Cycladic Massif (e.g., Löwen et al. 2015). The 1.1–1.6 Ga age gap excludes the Amazonian Craton (west Gondwana) and the Baltic shield as the source area for the studied quartzites. In contrast, the Sahara Metacraton could be a potential source area for the Ediacaran, Cryogenian, Paleoproterozoic, and Archean detrital zircons. Neoarchean and Paleoproterozoic cratonic domains of the Sahara Metacraton basement have been overprinted by deformation, metamorphism, and emplacement of igneous bodies during Neoproterozoic remobilization, associated with the assembly of east Gondwana (e.g., Stern 1994; Meert and van der Voo 1997; Abdelsalam et al. 2002; Küster et al. 2008). The predominant Cryogenian/Ediacaran age peaks at 580–640 Ma observed in the PQ unit s.s. could be explained by invoking sourcing from the east African orogen with its juvenile crust of the Arabian–Nubian shield (Finger et al. 2008 and references therein). However, east Africa cannot have been the source of late Ediacaran–Cambrian age zircons observed in the metasediments of the PQ unit s.s., because igneous activity was rare in this region after 570 Ma (Be'eri-Shlevin et al. 2009a; Avigad et al. 2012; Morag et al. 2011). A possible Cadomian provenance of the Ediacaran–Cambrian zircon grains can therefore be invoked.

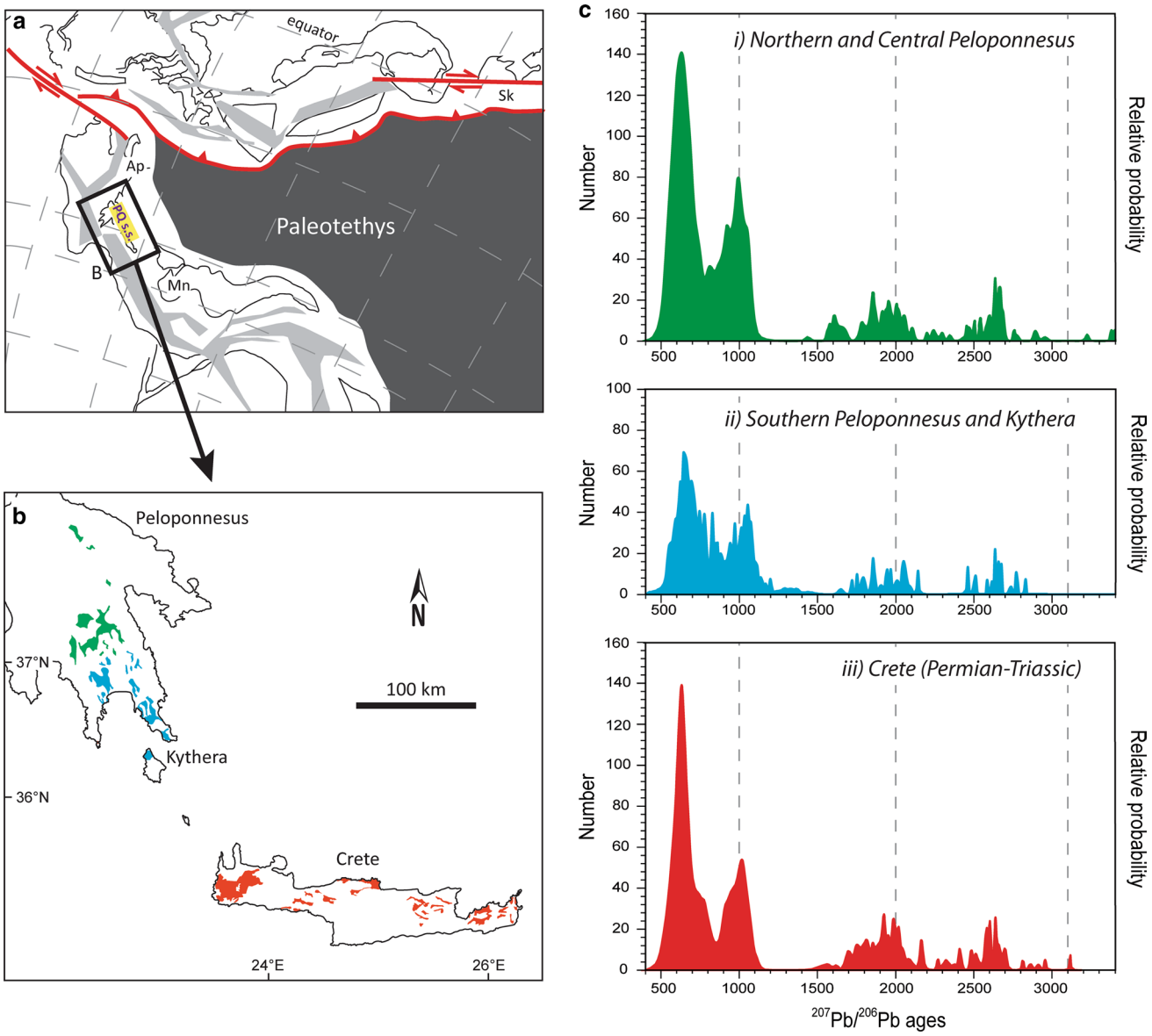

Fig. 6 **a** Paleogeographic map for the Permian (modified from Stamfli and Kozur 2006). The *light gray areas* are initial rift basin systems; the *rectangle* shows the position of Peloponnesus and Crete. Abbreviations *PQ s.s.* phyllite–quartzite unit sensu stricto, *Ap* apulia, *Mn* menderes, *Sk* sakarya. **b** Exposures of the PQ unit s.s. in the Peloponnesus, Kythera, and Crete. **c** Age spectra of the detrital zircons along the PQ unit s.s. Different colors correspond to the different parts of the PQ unit s.s. shown in (**b**). Data are: (i) northern and central Peloponnesus from this study; (ii) southern Peloponnesus and Kythera from Marsellos et al. (2012); (iii) Crete from Dörr et al. (2015), Zulauf et al. (this volume), and this study

The Stenian/Tonian age cluster at 0.9–1.1 Ga is more enigmatic compared to the rest. Cadomian-type terranes do not show evidence for Stenian/Tonian magmatism. Also, Stenian and Tonian zircons are restricted to the eastern margin of the Sahara Metacraton at the contact with the Arabian–Nubian Shield. The detrital zircons in the Cambrian sediments of northeast Africa and the Arabian Platform (Be'eri-Shlevin et al. 2009b) can be explained by recycling of Cryogenian/Tonian metasediments. Such metasediments could be present along the eastern margin of the Sahara Metacraton and the northern margin of the Arabian–Nubian shield. This recycling of metasediments could be combined with erosion of the Bayuda basement in northern Sudan and the Sa'al metamorphic complex in south Sinai (Dörr et al. 2015). The occurrence of the Stenian/Tonian detrital zircons in the siliciclastic metasediments of the PQ unit s.s. could be the result of fluvial transport within the Gondwana Super-fan System (Squire et al. 2006) from the Kibaran basement of the Transgondwanan Supermountain. This scenario requires significant transport toward the northeastern

Gondwana margin during the early Paleozoic (Zulauf et al. 2007; Morag et al. 2011; Meinhold et al. 2012; Kydonakis et al. 2014). The fact that northeast Africa and the eastern peri-Gondwana terranes lack any record of 1.3 Ga zircons, present in the Kibaran basement, renders this scenario less favorable. Dörr et al. (2015) proposed an alternative scenario, which involves provenance of the detrital zircons from the recently discovered Stenian/Tonian basement in the northern Arabian–Nubian shield (Sinai, Be'eri-Shlevin et al. 2012). This scenario is in agreement with the interpretation of the angular Tonian zircons in the Cambrian sediments of Israel as an indicator of a proximal source (Avigad et al. 2003).

In summary, the combination of: (1) low amount of metamorphic zircons in the source area; (2) the predominance of Cryogenian and Ediacaran zircons at similar amounts; (3) the high abundance of Stenian/Tonian zircons; (4) the Mesoproterozoic age gap; and (5) the existence of Precambrian zircons in the Permian to Triassic metasediments of the PQ unit s.s. favors an east Gondwana provenance.

Paleotectonic implications

The youngest detrital zircon age group in the PQ unit s.s. implies a late Cambrian maximum depositional age. A Cambro-Ordovician depositional age for the PQ unit s.s. has been proposed by Kydonakis et al. (2014). This Cambro-Ordovician depositional age is bracketed by their youngest concordant zircon age at 522 Ma and the drop in the sedimentation rates of the Gondwana Super-fan System around 460 Ma (Squire et al. 2006); the Gondwana Super-fan system is suggested to have provided the detritus of the PQ unit s.s. (Kydonakis et al. 2014). Fossil finds in the PQ unit s.s. on Crete suggest that the siliciclastic metasediments were deposited between the middle Carboniferous and Late Triassic (Krahl et al. 1983, 1986). No fossil older than middle Carboniferous has been found within the PQ unit s.s. (Krahl et al. 1983, 1986; Robertson 2006); it should be noted, however, that fossils are rare in the Peloponnesus. Assuming that the PQ unit s.s. on Crete and in the Peloponnesus are time-and-facies equivalent, a middle Carboniferous maximum depositional age for the PQ unit s.s. seems more plausible.

A striking feature of the detrital zircon age spectra is the complete absence of Ordovician to Triassic ages in all the quartzites of the PQ unit s.s. (Fig. 6c). The lack of Ordovician to Triassic zircons suggests that the depositional environment was isolated from Variscan and Early Triassic sources that dominate the detrital zircon record in the Cyclades (e.g., Löwen et al. 2015, and references therein). Therefore, Variscan (Devonian to Permian) and Triassic crystalline basement was not exposed in the source area of the siliciclastic sediments of the PQ unit s.s. This observation is in agreement with models placing the protolith of the PQ unit s.s. in a paleogeographic position south of the Paleotethys ocean, and along the northern margin of the Cimmerian continent or the Gondwana margin (Fig. 6a) (Dornsiepen et al. 2001; Stampfli et al. 2003; Stamfli and Kozur 2006; Kydonakis et al. 2014; Zulauf et al. 2015). In contrast, the pre-Alpine basement and the Tyros unit contain Carboniferous and Permian igneous rocks and related detrital zircons and therefore have been affected by Variscan orogenic imprints (Romano et al. 2004; Seidel et al. 2006; Xypolias et al. 2006; Zulauf et al. 2015). Therefore, the Paleotethys suture should be situated within the External Hellenides and in particular between the PQ unit s.s. and the Variscan pre-Alpine basement as has also been proposed by Kydonakis et al. (2014) and Zulauf et al. (2015, this volume). The PQ unit s.s. comprised the northern passive margin of Gondwana while the Variscan basement had a complex tectonometamorphic evolution at the northern Paleotethyan active margin. In places where the Variscan basement is lacking (e.g., in the northern and central Peloponnesus, and western Crete), the Paleotethys suture is portrayed by the contact between the PQ unit s.s. and the Tyros unit or the overlying Tripolitsa unit.

The significant amount of detrital zircon age data that are now available for the PQ unit s.s. provide important insights into: (1) the relationships between the siliciclastic sequences of the PQ unit s.s. exposed along the HP belt and (2) the paleogeographic configuration of the northern Gondwana margin during the late Paleozoic to early Mesozoic. In Fig. 6b, c, we compile detrital zircon ages that are available along the complete length of the P.Q. s.s. (Marsellos et al. 2012; Dörr et al. 2015; Zulauf et al. this volume; this study). The compiled data suggest that the Permian–Triassic quartzites—ages based on biostratigraphic data—on Crete have similar detrital zircon age spectra with the quartzites of unknown age on Kythera and the Peloponnesus. The age spectra from the southern Peloponnesus and Kythera have the same—but less well defined—age peaks compared to those from Crete and northern/central Peloponnesus. The consistency of the detrital zircon age spectra along the 600 km exposure of the PQ unit s.s. favors a common paleogeographic origin for the siliciclastic metasediments on Crete, Kythera, and the Peloponnesus; their protoliths were lateral equivalents and parts of the same sequence deposited in a paleogeographic area situated along the northern Gondwana margin. The source of the detritus that were deposited in the paleogeographic area of the PQ unit s.s. protolith remained constant in space and time during the Paleozoic–early Mesozoic. Paleotectonic models of dextral terrane transport along the northern Gondwana margin during Carboniferous–Permian (Robertson 2006) or Permian–Triassic (Dornsiepen et al. (2001) do not reconcile with the detrital zircon data from the PQ unit s.s. These models suggest

juxtaposition of crustal fragments with diverse affinities and siliciclastic sequences of diverse provenance, which is not supported by the spatiotemporal consistency of the detrital zircon age spectra in the PQ unit s.s.

Conclusions

New detrital zircon U–Pb data from quartzites of the PQ unit s.s. in the External Hellenides allow us to draw the following conclusions:

1. The detrital zircon age spectra remain largely consistent between the different tectonostratigraphic levels of the PQ unit s.s. The Permian–Triassic quartzites on Crete show similar age spectra with the quartzites of unknown age on Kythera and the Peloponnesus. Therefore, the siliciclastic sequences of the PQ unit s.s. have a common paleogeographic origin and are characterized by a spatiotemporally consistent source of detritus along the HP belt in the External Hellenides.
2. The Neoproterozoic ages predominate the age spectra; Ediacaran and Cryogenian zircons comprise the dominant populations, while Stenian/Tonian zircons are present in a smaller amount. A pronounced age peak exists at ca. 600 Ma and a smaller peak at ca. 1000 Ma. These peaks are typical for east Gondwana provenance.
3. The Saharan Metacraton and the Arabian–Nubian shield could be the source of the Ediacaran, Cryogenian, Stenian/Tonian, Paleoproterozoic and Archean zircons. A Cadomian provenance can be invoked for the Ediacaran/Cambrian zircon grains.
4. The lack of Carboniferous to Triassic ages in the analyzed quartzites of the PQ unit s.s. suggests a depositional environment restricted from Variscan and early Mesozoic sources. The protolith of the PQ unit s.s. was therefore deposited in a paleogeographic area south of the Paleotethys ocean and along the northern Gondwana margin.

Acknowledgments We thank Michael Bröcker and an anonymous reviewer for their constructive comments. This work was financially supported by a common grant of IKY (Greek State Scholarships Foundation) and DAAD (IKYDA2012). V.C. acknowledges financial support from the Greek State Scholarships Foundation for fieldwork and thanks Zach Michels for suggestions on the text.

References

Abdelsalam MG, Liégeois JP, Stern RJ (2002) The Saharan Metacraton. J Afr Earth Sci 34:119–136

Anders B, Reischmann T, Kostopoulos D, Poller U (2006) The oldest rocks of Greece: first evidence for a Precambrian terrane within the Pelagonian Zone. Geol Mag 143:41–58

Avigad D, Kolodner K, McWilliams M, Persing H, Weissbrod T (2003) Origin of northern Gondwana Cambrian sandstone revealed by detrital zircon SHRIMP dating. Geology 31:227–230

Avigad D, Gerdes A, Morag N, Bechstadt T (2012) Coupled U–Pb–Hf of detrital zircons of Cambrian sandstones from Morocco and Sardinia: implications for provenance and Precambrian crustal evolution of north Gondwana. Gondwana Res 21:690–703

Be'eri-Shlevin Y, Katzir Y, Whitehouse M (2009a) Post-collisional tectonomagmatic evolution in the northern Arabian-Nubian Shield: time constraints from ion-probe U–Pb dating of zircon. J Geol Soc Lond 166:71–85

Be'eri-Shlevin Y, Katzir Y, Whitehouse MJ, Kleinhanns IC (2009b) Contribution of pre Pan-African crust to formation of the Arabian Nubian Shield: new secondary ionization mass spectrometry U–Pb and O studies of zircon. Geology 37:899–902

Be'eri-Shlevin Y, Eyal M, Eyal Y, Whitehouse MJ, Litvinovsky B (2012) The Sa'al volcano-sedimentary complex (Sinai, Egypt): a latest Mesoproterozoic volcanic arc in the northern Arabian Nubian Shield. Geology 40:403–406

Bizon G, Thiebault F (1974) Données nouvelles sur l' âge des marbres et quartzites u Taygéte (Péloponnèse neridional Grèce). C R Acad Sci 278:9–12

Blumör T (1998) Die Phyllit-Quarzit-Serie SE-Lakoniens (Peloponnes, Griechenland): Hochdruckmetamorphite in einem orogenen Keil. Frankf. Geowiss. Arb. A17:187 pp

Bonneau M (1984) Correlation of the Hellenide nappes in the southeast Aegean and their tectonic reconstruction. In: Dixon JE, Robertson AHF (eds) The Geological Evolution of the Eastern Mediterranean. Geol Soc Lond Spec Publ 17:517–527

Chatzaras V, Xypolias P, Doutsos T (2006) Exhumation of high-pressure rocks under continuous compression: a working hypothesis for the southern Hellenides (central Crete, Greece). Geol Mag 143:859–876

Chatzaras V, Xypolias P, Kokkalas S, Koukouvelas I (2013a) Tectonic evolution of a crustal-scale oblique ramp, Hellenides thrust belt. Greece J Struct Geol 57:16–37

Chatzaras V, Dörr W, Finger F, Xypolias P, Zulauf G (2013b) U–Pb single zircon ages and geochemistry of metagranitoid rocks in the Cycladic Blueschists (Evia Island): implications for the Triassic tectonic setting of Greece. Tectonophysics 595–596:125–139

Dornsiepen UF, Manutsoglu E, Mertmann D (2001) Permian-Triassic palaeogeography of the external Hellenides. Palaeo 172:327–338

Dörr W, Zulauf G, Gerdes A, Lahayec Yann, Kowalczyk Gotthardt (2015) A hidden Tonian basement in the eastern Mediterranean: age constraints from U–Pb data of magmatic and detrital zircons of the External Hellenides (Crete and Peloponnesus). Precambrian Res 258:83–108

Doutsos T, Koukouvelas I, Poulimenos G, Kokkalas S, Xypolias P, Skourlis K (2000) An exhumation model of the south Peloponnesus. Greece Int J Earth Sci 89:350–365

Epting M, Kudrass H-R, Schäfer A (1972) Stratigraphie et position des séries métamorphiques aux Talea Ori/Créte. Z Deut Ges Geowiss 123:365–370

Fassoulas C, Kilias A, Mountrakis D (1994) Post-nappe stacking extension and exhumation of the HP/LT rocks in the island of Crete, Greece. Tectonics 13:127–138

Finger F, Krenn E, Riegler G, Romano S, Zulauf G (2002) Resolving Cambrian, Carboniferous, Permian and Alpine monazite generations in the polymetamorphic basement of eastern Crete (Greece) by means of the electron microprobe. Terra Nova 14:233–240

Finger F, Dörr W, Gerdes A, Gharib M, Dawoud M (2008) U–Pb zircon ages and geochemical data for the Monumental Granite and other granitiod rocks from Aswan, Egypt: implications for the geological evolution of the Arabian Nubian Shield. Mineral Petrol 93:153–183

Fortuin AR (1978) Late Cenozoic history of eastern Crete and implications for the geology and geodynamics of the southern Aegean area. Geol Mijnb 57:451–464

Frei D, Gerdes A (2008) Accurate and precise in situ zircon U–Pb age dating with high spatial resolution and high sample throughput by automated LA-SF-ICP-MS. Chem Geol 261:261–270

Fu B, Bröcker M, Ireland T, Holden P, Kinsley LPJ (2015) Zircon U– Pb, O, and Hf isotopic constraints on Mesozoic magmatism in the Cyclades, Aegean Sea, Greece. Int J Earth Sci 104:75–87

Gerolymatos IK (1994) Metamorphose und Tektonik der Phyllit-Quarzit-Serie und der Tyros-Schichten auf dem Peloponnes und Kythira. Berliner Geowiss. Abh. 164:101 pp., Berlin

Harley SL, Kelly NM (2007) Zircon tiny but timely. Elements 3:13–18

Hartmann LA, Santos JOS (2004) Predominance of high Th/U, magmatic zircon in Brazilian Shield sandstones. Geology 32:73–76

Himmerkus F, Anders B, Reischmann T, Kostopoulos D (2007) Gondwana-derived terranes in the northern Hellenides. Geol Soc Am Mem 200:379–390

Jackson SE, Pearson NJ, Griffin WL, Belousova EA (2004) The application of laser ablation-inductively coupled plasma-mass spectrometry to in situ U–Pb zircon geochronology. Chem Geol 211:47–69

Jolivet L, Trotet F, Monié P, Vidal O, Goffé B, Labrousse L, Agard P, Ghorbal B (2010) Along-strike variations of P-T conditions in accretionary wedges and syn-orogenic extension, the HP–LT Phyllite-Quartzite Nappe in Crete and the Peloponnese. Tectonophysics 480:133–148

Katagas C, Tsolis-Katagas P, Baltatzis E (1991) Chemical mineralogy and illite crystallinity in low grade metasediments, Zarouchla Group, Northern Peloponnesus. Greece Mineral Petrol 44:57–71

Kirkland CL, Smithies RH, Taylor RJM, Evans N, McDonald B (2015) Zircon Th/U ratios in magmatic environs. Lithos 212–215:397–414

Klein T, Craddock JP, Zulauf G (2013) Constraints on the geodynamical evolution of Crete: insights from illite crystallinity, Raman spectroscopy and calcite twinning above and below the "Cretan Detachment". Int J Earth Sci 102:139–182

Konstantopoulos PA, Maravelis AG, Zelilidis A (2013) The implication of transfer faults in foreland basin evolution: application on Pindos foreland basin, West Peloponnesus, Greece. Terra Nova 25:323–336

Krahl J, Kauffmann G, Kozur H, Richter D, Forster O, Heinritzi F (1983) Neue Daten zur Biostratigraphie and zur tektonischen Lagerung der Phyllit-Gruppe und der Trypali-Gruppe auf der Insel Kreta (Griechenland). Geol Rundsch 72:1147–1166

Krahl J, Kauffmann G, Richter D, Kozur H, Möller I, Förster O, Heinritzi F, Dornsiepen U (1986) Neue Fossilfunde in der Phyllit-Gruppe Ostkretas (Griechenland). Z Deut Geol Ges 137:523–536

Küster D, Liégeois J-P, Matukov D, Sergeev S, Lucassen F (2008) Zircon geochronology and Sr, Nd, Pb isotope geochemistry of granitoids from Bayuda Desert and Sabaloka (Sudan): evidence for a Bayudian event (920–900 Ma) pre- ceding the Pan-African orogenic cycle (860–590–Ma) at the eastern boundary of the Saharan Metacraton. Precambrian Res 164:16–39

Kydonakis K, Kostopoulos D, Poujol M, Brun J-P, Papanikolaou D, Paquette J-L (2014) The dispersal of the Gondwana Super-fan System in the eastern Mediterranean: new insights from detrital zircon geochronology. Gondwana Res 5:1230–1241

Linnemann U, Ouzegane K, Drareni A, Hofmann M, Becker S, Gärtner A, Sagawe A (2011) Sands of West Gondwana: an archive of secular magmatism and plate interactions—a case study from the Cambro-Ordovician section of the Tassili Ouan Ahaggar (Algerian Sahara) using U–Pb LA-ICP-MS detrital zircon ages. Lithos 123:188–203

Lode S, Romer T, Völs S, Xypolias P, Zulauf G (2008) The pre-Alpine basement of Kythira (Greece). In: Xypolias P, Zulauf G (eds) New results and concepts on the regional geology of the eastern mediterranean. Z Deut Ges Geowiss 159:457–468

Löwen K, Bröcker M, Berndt J (2015) Depositional ages of clastic metasediments from Samos and Syros, Greece: results of a detrital zircon study. Int J Earth Sci 104:205–220

Ludwig KR (1994) Isoplot—a plotting and regression program for radiogenic- isotope data. Version 2.75: US Geological Survey Open-File Report 91–445

Maravelis A, Panagopoulos G, Piliotis I, Pasadakis N, Manoutsoglou E, Zelilidis A (2013) Pre-messinian (sub-salt) source-rock potential on back-stop basins of the hellenic trench system (Messara Basin, Central Crete, Greece). Oil Gas Sci Technol. doi:10.2516/ogst/2013130

Marsellos AE, Kidd WSF, Garver JI (2010) Extension and exhumation of the HP/LT rocks in the Hellenic forearc ridge. Am J Sci 310:1–36

Marsellos AE, Foster DA, Kamenov GD, Kyriakopoulos K (2012) Detrital zircon U–Pb data from the Hellenic south Aegean belts: constraints on the age and source of the South Aegean basement. J Virt Expl 42. doi:10.3809/jvirtex.2011.00284 (paper 3)

Meert JG, van der Voo R (1997) The assembly of Gondwana 800–550 Ma. J Geodyn 23:223–235

Meinhold G, Kostopoulos D, Frei D, Himmerkus F, Reischmann T (2010) U–Pb LASF-ICP-MS zircon geochronology of the Serbo-Macedonian Massif, Greece: palaeotectonic constraints for Gondwana-derived terranes in the Eastern Mediterranean. Int J Earth Sci 99:813–832

Meinhold G, Morton AC, Avigad D (2012) New insights into peri-Gondwana paleogeography and the Gondwana super-fan system from detrital zircon U–PbU–Pb ages. Gondwana Res 23:661–665

Moix P, Beccaletto L, Kozur HW, Hochard C, Rosselet F, Stampfli GM (2008) A new classification of the Turkish terranes and its implication for paleotectonic history of the region. Tectonophysics 451:7–39

Möller A, O'Brien PJ, Kennedy A, Kroner A (2002) Polyphase zircon in ultrahigh- temperature granulites (Rogaland, SW Norway): constraints for Pb diffusion in zircon. J Metamorph Geol 20:727–740

Morag N, Avigad D, Gerdes A, Belousova E, Harlavan Y (2011) Detrital zircon Hf isotopic composition indicates long-distance transport of north Gondwana Cambrian-Ordovician sandstones. Geology 39:955–958

Murphy JB, Pisarevsky SA, Nance RD, Keppie JD (2004) Neoproterozoic-Early Palaeozoic evolution of peri-Gondwanan terranes: implications for Laurentia-Gondwana connections. Int J Earth Sci 93:659–682

Nance RD, Murphy JB (1996) Basement isotopic signatures and Neoproterozoic paleogeography of Avalonian-Cadomian and related terranes in the circum-North Atlantic. In: Nance RD, Thompson MD (eds) Avalonian and Related Peri-Gondwanan Terranes of the Circum-North Atlantic. Geol Soc Am Spec Pap 304:333–346

Nasdala L, Hofmeister W, Norberg N, Mattinson JM, Corfu F, Dörr W, Kamo SL, Kennedy AK, Kronz A, Reiners PW, Frei D, Kosler J, Wan Y, Götze J, Häger T, Kröner A, Valley JW (2008) Zircon M257—a Homogeneous natural reference material for the Ion Microprobe U–Pb analysis of zircon. Geostand Geoanal Res 32:247–265

Papanikolaou DJ, Skarpelis NS (1987) The blueschists in the external metamorphic belt of the Hellenides: composition, structure and geotectonic significance of the Arna Unit. Ann Geol Pays Hell 33:47–68

Papanikolaou D, Vassilakis E (2010) Thrust faults and extensional detachment faults in Cretan tectono-stratigraphy: implications for Middle Miocene extension. Tectonophysics 488:233–247

Passchier CW, Trouw RAJ (2005) Microtectonics. Springer, Berlin

Robertson AHF (2006) Sedimentary evidence from the south Mediterranean region (Sicily, Crete, Peloponnese, Evia) used to test alternative models for the regional tectonic setting of Tethys during Late Palaeozoic–Early Mesozoic time. In: Robertson AHF, Mountrakis D (eds) Tectonic development of the eastern mediterranean region. Geol Soc Lond Spec Publ 260:91–154

Robertson AHF (2007) Overview of tectonic settings related to the rifting and opening of Mesozoic ocean basins in the Eastern Tethys: Oman, Himalayas and Eastern Mediterranean regions. In: Karner G, Manatschal G, Pinheiro L (eds) Imaging, mapping and modelling continental lithosphere extension and breakup: Geol Soc Lond Spec Public 282:325–389

Robertson AHF (2008) Late Palaeozoic-Early Mesozoic metasedimentary and metavolcanic rocks of the Phyllite-Quartzite Unit, eastern Crete (Greece): an extensional, rift-related setting for the southern margin of Tethys in the Eastern Mediterranean region. Z Deut Ges Geowiss 159:351–374

Robertson AHF, Dixon JE, Brown S, Collins A, Morris A, Pickett EA, Sharp I, Ustaömer T (1996) Alternative tectonic models for the Late Palaeozoic–Early Tertiary development of Tethys in the Eastern Mediterranean region. In: Morris A, Tarling DH (eds) Palaeomagnetism and tectonics of the mediterranean region: Geol Soc Lond Spec Publ 105:239–263

Romano SS, Dörr W, Zulauf G (2004) Total Pb loss of Cadomian zircons due to Alpine subduction: examples from the pre-Alpine basement of Crete. In: Dörr W, Finger F, Linnemann U, Zulauf G (eds) The Avalonian-Cadomian Belt and related peri-Gondwanan terranes. Int J Earth Sci 93:844–859

Romano SS, Brix M, Dörr W, Fiala J, Krenn E, Zulauf G (2006) The Carboniferous to Jurassic evolution of the pre-Alpine basement of Crete: constraints from radiometric dating of orthogneiss, fission-track dating of zircon and structural/petrological data. Geol Soc Lond Spec Publ 260:69–90

Romer T, Völs S, Schulz B, Xypolias P, Zulauf G, Krenn E (2008) Metamorphism and P–T paths of the pre-Alpine basement and the Phyllite-Quartzite unit s.str. of Kythira (External Hellenides, Greece). In: Xypolias P, Zulauf G (eds) New results and concepts on the regional geology of the eastern mediterranean. Z Deut Ges Geowiss 159:469–484

Rubatto D, Williams IS, Buick IS (2001) Zircon and monazite response to prograde metamorphism in the Reynolds Range, central Australia. Contr Mineral Petrol 140:458–468

Samson SD, D'Lemos RS, Miller BV, Hamilton MA (2005) Neoproterozoic palaeogeography of the Cadomia and Avalon terranes: constraints from detrital zircon U–Pb ages. J Geol Soc Lond 162:65–71

Seidel E (1978) Zur Petrologie der Phyllit-Quarzit-Serie Kretas. Habit-Schr Tech Univ, Braunschweig, pp 1–145

Seidel E, Kreuzer H, Harre W (1982) A late Oligocene/early Miocene high pressure belt in the external Hellenides. Geol Jahrb E 23:165–206

Seidel M, Zacher W, Schwarz WH, Jaeckel P, Reischmann T (2006) A Late Carboniferous age of the gneiss of Potamos (Kythira Island, Greece) and new considerations on geodynamic interpretations of the Western Hellenides. Neues Jahrb Geol Paläontol Abh 241:325–344

Şengör AMC, Yılmaz Y, Sungurlu O (1984) Tectonics of the Mediterranean Cimmerides: nature and evolution of the western termination of Palaeo-Tethys. In: Dixon JE, Robertson AHF (eds) The geological evolution of the eastern mediterranean. Geol Soc Lond Spec Publ vol 17, pp 77–112

Sláma J, Košler J, Condon DJ, Crowley JL, Gerdes A, Hanchar JM, Horstwood MSA, Morris GA, Nasdala L, Norberg N, Schaltegger U, Schoene B, Turbett MN, Whitehouse MJ (2008) Plešovice zircon: a new natural reference material for U–Pb and Hf isotopic microanalysis. Chem Geol 249:1–35

Squire RJ, Campbell IH, Allen CM, Wilson CJL (2006) Did the Transgondwanan Supermountain trigger the explosive radiation of animals on Earth? Earth Plan Sci Lett 250:116–133

Stacey JS, Kramers JD (1975) Approximation of terrestrial lead isotope evolution by a two-stage model. Earth Planet Sci Lett 26:207–221

Stamfli GM, Kozur HW (2006) Europe from the Variscan to the Alpine cycles. Memoirs Geol Soc Lond 32:57–82

Stampfli GM, Borel GD (2002) A plate tectonic model for the Paleozoic and Meso- zoic constrained by dynamic plate boundaries and restored synthetic oceanic isochrones. Earth Planet Sci Lett 196:17–33

Stampfli GM, von Raumer J, Borel GD (2002) The Paleozoic evolution of pre-variscan terranes: from peri-gondwana to the variscan collision. In: Martinez-Catalan JR, Hatcher RD, Arenas R, Diaz Garcia F (eds) Variscan appalachian dynamics: the building of the Upper Paleozoic basement. Geol Soc Am Spec Pap 364:263–280

Stampfli G, Vavassis I, De Bono A, Rosselet F, Matti B, Bellini M (2003) Remnants of the Paleotethys oceanic suture-zone in the western Tethyan area. Stratigraphic and structural evolution on the Late Carboniferous to Triassic Continental and Marine Successions in Tuscany (Italy): regional reports and general correlation. Boll Soc Geol It 2:1–24

Stern RJ (1994) Arc assembly and continental collision in the Neoproterozoic East African Orogen: implications for the assembly of Gondwanaland. Annu Rev Earth Planet Sci 22:319–351

Teipel U, Eichhorn R, Loth G, Rohrmüller J, Höll R, Kennedy A (2004) U–Pb SHRIMP and Nd isotopic data from the western Bohemian Massif (Bayerischer Wald, Germany): implications for Upper Vendian and Lower Ordovician magmatism. Int J Earth Sci 93:782–801

Theye T (1988) Aufsteigende Hochdruckmetamorphose in Sedimenten der Phyllit-Quartzit-Einheit Kretas und des Peloponnes. Dissertation, Tech Univ, Braunschweig, pp 1–224

Theye T, Seidel E (1991) Petrology of low-grade high-pressure metapelites from the External Hellenides (Crete Peloponnese): a case study with attention to sodic minerals. Eur J Mineral 3:343–366

Theye T, Seidel E, Vidal O (1992) Carpholite, sudoite, and chloritoid in low-grade high-pressure metapelites from Crete and the Peloponnese. Eur J Mineral 4:487–507

Thiebault F, Triboulet T (1984) Alpine metamorphism and deformation in Phyllite nappes (external Hellenides southern Peloponnesus Greece): geodynamic implication. J Geol 92:185–199

van Hinsbergen DJJ, Meulenkamp JE (2006) Neogene supradetachment basin development on Crete (Greece) during exhumation of the South Aegean core complex. Basin Res 18:103–124

von Raumer JF (1998) The Palaeozoic evolution in the Alps: from Gondwana to Pangea. Geol Rundsch 87:407–435

Wiedenbeck M, All P, Corfu F, Griffin WL, Meier M, Oberli F, von Quadt A, Roddick JC, Spiegel W (1995) Three natural zircon standards for U-Th–Pb, Lu–Hf, trace elements and REE analyses. Geostand Newsl 19:1–23

Williams IS, Buick IS, Cartwright I (1996) An extended episode of early Mesoproterozoic metamorphic fluid flow in the Reynolds Range, Central Australia. J Metamorph Geol 14:29–47

Xypolias P, Doutsos T (2000) Kinematics of rock flow in a crustal-scale shear zone: implication for the orogenic evolution of the southwestern Hellenides. Geol Mag 137:81–96

Xypolias P, Kokkalas S (2006) Heterogeneous ductile deformation along a mid- crustal extruding shear zone: an example from the External Hellenides (Greece). In: Law RD, Searle M, Godin L (eds) Channel flow, ductile extrusion and exhumation in continental collision zones. Geol Soc Lond Spec Publ 268:497–516

Xypolias P, Koukouvelas I (2001) Kinematic vorticity and strain rate patterns associated with ductile extrusion in the Chelmos Shear zone (External Hel-lenides, Greece). Tectonophysics 338:59–77

Xypolias P, Dörr W, Zulauf G (2006) Late Carboniferous plutonism within the pre-Alpine basement of the External Hellenides (Kithira, Greece): evidence from U–Pb zircon dating. J Geol Soc Lond 163:539–547

Xypolias P, Koukouvelas I, Zulauf G (2008) Cenozoic tectonic evolution of northeastern Apulia: insights from a key study area in the Hellenides (Kythira, Greece). Z Deut Ges Geowiss 159:439–455

Zachariasse WJ, van Hinsbergen DJ, Fortuin AR (2011) Formation and fragmentation of a late Miocene supradetachment basin in central Crete: implications for exhumation mechanisms of high-pressure rocks in the Aegean forearc. Basin Res 23:678–701

Zlatkin O, Avigad D, Gerdes A (2013) Evolution and provenance of Neoproterozoic basement and Lower Paleozoic siliciclastic cover of the Menderes Massif (western Taurides): coupled U–Pb–Hf zircon isotope geochemistry. Gondwana Res 23:682–700

Zulauf G, Kowalczyk G, Petschick R, Schwanz S, Krahl J (2002) The tectonometamorphic evolution of high-pressure low-temperature metamorphic rocks of eastern Crete, Greece: constraints from microfabrics, strain, illite crystallinity and paleostress. J Struct Geol 24:1805–1828

Zulauf G, Dörr W, Fiala J, Romano SS (2007) Crete and the Minoan Terranes: age constraints from U–Pb dating of detrital zircons. In: Linnemann U, Nance RD, Kraft P, Zulauf G (eds) The evolution of the rheic ocean: from avalonian to cadomian active margin to alleghenian-variscan collission. Geol Soc Am Spec Pap 423:401–409

Zulauf G, Klein T, Kowalczyk G, Krahl J, Romano S (2008). The Mirsini syncline of eastern Crete, Greece: a key area for understanding pre-Alpine and Alpine orogeny in the eastern Mediterranean. In: Xypolias P, Zulauf G (Ees) New results and concepts on the regional geology of the eastern mediterranean. Z Deut Ges Geowiss 159:399–414

Zulauf G, Blau J, Dörr W, Klein T, Krahl J, Kustatscher E, Petschick R, van de Schootbrugge B (2013) New U–Pb zircon and biostratigraphic data of the Tyros Unit, eastern Crete: constraints on Triassic palaeogeography and depositional environment of the eastern Mediterranean. Z Deut Ges Geowiss 164:337–352

Zulauf G, Dörr W, Fisher-Spurlock SC, Gerdes A, Chatzaras V, Xypolias P (2015) Closure of the Paleotethys in the External Hellenides: constraints from U–Pb ages of magmatic and detrital zircons (Crete). Gondwana Res 28:642–667